Determination of the spin polarization of a $^4He^+$ ion beam

T. Suzuki[1,2,*] and Y. Yamauchi[1]
[1]*National Institute for Materials Science, 1-2-1 Sengen, Tsukuba, Ibaraki 305-0047, Japan*
[2]*PRESTO, Japan Science and Technology Agency, 5-Sanbancho, Chiyodaku, Tokyo 102-0075, Japan*
(Received 27 November 2007; published 12 February 2008)

It was demonstrated that the spin polarization of a $^4He^+$ ion beam (P_{He^+}) can be determined from the spin dependence of the electron emission in the deexcitation process of spin-polarized He metastable atoms (He^*, $2\,^3S_1$) and spin-polarized He^+ ions on Fe (100) surfaces. On Fe (100) surfaces, both He^* and He^+ deexcite via Auger neutralization, and therefore, the spin asymmetry obtained from spin-polarized He^+ ion neutralization spectroscopy should be equal to that from spin-polarized metastable He^* deexcitation spectroscopy. The spin polarization of He^* was obtained from Stern-Gerlach measurements. P_{He^+} was finally determined to be 0.19 ± 0.02.

DOI: 10.1103/PhysRevA.77.022902 PACS number(s): 79.20.Rf, 34.80.Nz, 29.25.Lg

I. INTRODUCTION

The recently developed electron spin-polarized $^4He^+$ ion beam can be a probe for surface and interface magnetism (spin states) [1,2]. Most of the impinging He^+ ions on sample surfaces with low kinetic energy (<keV) are neutralized. This is because the ionization energy of He is much larger than the work function of solid surfaces, and consequently, Auger neutralization (AN) occurs efficiently. The larger scattering cross section with lower kinetic energy of projectiles is another reason for the surface sensitivity of low-energy He^+ ion beams. The sensitivity of the spin-polarized He^+ ion beam to the surface magnetism of samples depends on the spin polarization of the beam (P_{He^+}). Thus, great efforts have been made to improve P_{He^+}, although it has been demonstrated that an unpolarized He^+ ion beam can also detect surface magnetism [3,4]. For example, Bixler and coworkers have improved P_{He^+} by using an intense source of optical pumping (OP) radiation [5]. Very recently, we reported improvement of P_{He^+} by OP using circularly and linearly polarized radiation tuned to the D_0 line [He metastable atoms (He^*), $2\,^3S_1 \rightarrow 2\,^3P_0$] [6].

One of the problems in developing a spin-polarized He^+ ion source has been the lack of a well-established method to determine P_{He^+}. In a pioneering work by Bixler and coworkers, P_{He^+} was measured from the spin correlation between two electrons involved in AN, which is a predominant neutralization process of He^+ ions on an Au(100) surface [7]. Briefly, it was empirically derived that if the surface electron filling the hole of He^+ $1s$ is perfectly spin-polarized (i.e., polarization of 1.0), the spin polarization of electrons emitted from the Au (100) surface is 0.3. Then, P_{He^+} is inferred from the spin polarization of the emitted electrons (P_e) measured by a Mott polarimeter as $P_e/0.3$.

In the present study, we develop a method to determine P_{He^+}. Our method is based on a comparison of the spin dependence of the electron spectra between He^* and He^+. In other words, spin asymmetries obtained from spin-polarized metastable deexcitation spectroscopy (SPMDS) and spin-polarized ion neutralization spectroscopy (SPINS) are compared to determine P_{He^+}.

It is well known that He^* approaching clean Fe surfaces is ionized by a tunneling of the He^* $2s$ electron into the unoccupied states of the surface (resonance ionization) [8]. The subsequent deexcitation process of the ionized He^*—i.e., He^+—should be the same as that of projectiles with the original state as He^+ for which the dominant neutralization process on clean Fe surfaces is AN [9]. Thus, the mechanism of electron emission is considered to be basically the same for SPINS and SPMDS on Fe surfaces.

The spin asymmetry of SPMDS (A_{MDS}) is expressed as

$$A_{MDS} = \frac{I^{\uparrow}_{MDS} - I^{\downarrow}_{MDS}}{P_{He^*}(I^{\uparrow}_{MDS} + I^{\downarrow}_{MDS})}, \tag{1}$$

where $I^{\uparrow}_{MDS}$ and $I^{\downarrow}_{MDS}$ are the emitted electron intensity by He^* with up and down spins, respectively. P_{He^*} is the spin polarization of the He^* beam, and it can be experimentally obtained from Stern-Gerlach measurements as described later. Similarly, the spin asymmetry of SPINS (A_{INS}) is expressed as

$$A_{INS} = \frac{I^{\uparrow}_{INS} - I^{\downarrow}_{INS}}{P_{He^+}(I^{\uparrow}_{INS} + I^{\downarrow}_{INS})}, \tag{2}$$

where $I^{\uparrow}_{INS}$ and $I^{\downarrow}_{INS}$ are the emitted electron intensity by He^+ with up and down spins, respectively. If the electron emission mechanism is identical between SPINS and SPMDS as expected, A_{MDS} should agree with A_{INS}. Then, P_{He^+} is obtained as

$$P_{He^+} = \frac{I^{\uparrow}_{INS} - I^{\downarrow}_{INS}}{A_{MDS}(I^{\uparrow}_{INS} + I^{\downarrow}_{INS})}. \tag{3}$$

All variables on the right-hand side of Eq. (3) can be obtained, and thus P_{He^+} is expected to be experimentally determined.

We have already briefly reported the essence of the method to determine P_{He^+} [10]. However, as a result of slight oxygen contamination on Fe surfaces, a different deexcitation process (Auger deexcitation) was involved in that study, and consequently, substantial ambiguity arose in the determi-

*Corresponding author: suzuki.taku@nims.go.jp

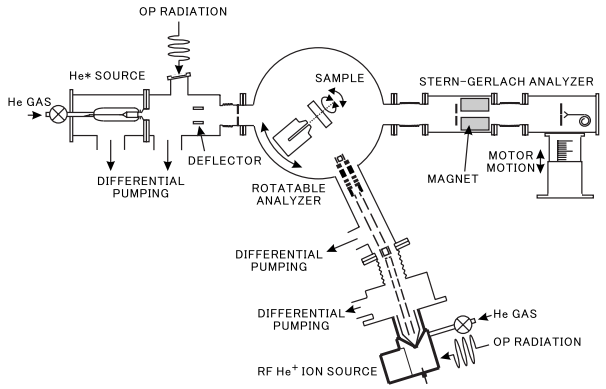

FIG. 1. Schematic of the experimental setup.

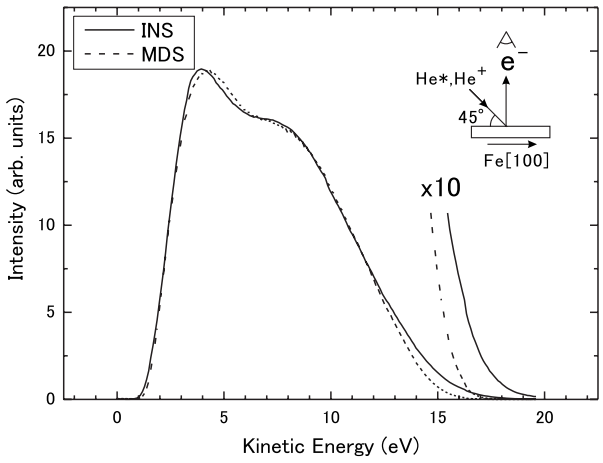

FIG. 2. INS and MDS spectra on the Fe (100) surface. The incidence angle of the projectile and exit angle of electrons are 45° and 0°, respectively, for both INS and MDS.

nation of P_{He^+}. In the present study, the Fe (100) clean surface was carefully prepared to realize the identical deexcitation process between He^+ and He^*. The important role of the kinetic energy of He^* and He^+ in the comparison of MDS and INS is found in the present study. Accordingly, a reasonable correction of the spectra is necessary in a direct comparison between MDS and INS to compensate for the effect of the kinetic energy of projectiles. This paper proposes a method of the correction, whose validity is confirmed from a comparison of the spin asymmetry curves of MDS and INS in the present study.

In the beginning part of the present paper, the electron emission mechanism by impinging He^* and He^+ on Fe surfaces will be discussed. It is observed that the energy of the high-energy cutoff of INS spectra on Fe (100) is slightly larger than that of MDS spectra. This is attributed to the difference of the kinetic energy between He^+ (~14 eV) and He^* (~0.2 eV). The spin asymmetry spectra of SPMDS and SPINS are finally compared to determine P_{He^+}.

II. EXPERIMENT

Figure 1 shows a schematic of our experimental setup. The experiments were performed in an ultrahigh-vacuum chamber (base pressure $\sim 5\times 10^{-11}$ Torr), which was equipped with a rotatable hemispherical sector analyzer (Omicron, SHA50), a beam line for spin-polarized He^*, a Stern-Gerlach analyzer, a beam line for spin-polarized He^+, an ion gun for sample cleaning, an optics of reflection high-energy electron diffraction, and an Fe deposition source.

In the measurement of (SP)MDS, the discharge was pulsed to separate photons and He^* by a time-of-flight technique [11]. A 1083-nm radiation with circular polarization tuned to the D_1 line (He^*, $2\,^3S_1 \rightarrow 2\,^3P_0$) from a laser diode (SDL 6702) was utilized for OP to generate a spin-polarized He^* beam [12,13]. Ions contained in the beam were removed by an electrostatic deflector placed between the sample and the OP region. The spin polarization of He^* was measured by a Stern-Gerlach analyzer.

A spin-polarized He^+ ion beam was generated from a rf ion source irradiated by a 1083-nm laser light (D_1 line) with circular polarization. Although we have shown that a higher P_{He^+} is obtained by using the D_0 line [6], the D_1 line was used in OP to compare with former studies, which utilized the D_1 line in OP. The details of the spin-polarized He^+ beam line and the arrangement of the optical components for OP have been described elsewhere [6,10]. Briefly, spin-polarized He^+ ions are generated from Penning ionization of spin-polarized He^*. The spin angular momentum is conserved in the Penning ionization, and thus, if He^* is spin polarized by OP, spin-polarized He^+ ions are generated [5]. The typical rf power and the He pressure in the source were 1 W and 20 Pa, respectively. All the electrodes in the He^+ beam line are electrically floated, and He^+ ions are decelerated just in front of the sample to obtain high current density. The He^+ beam line is deflected by 3° to eliminate neutral particles, such as photons, fast He^0 neutrals, and He^*.

Iron single-crystalline (100) films (bcc Fe) were epitaxially grown on MgO (100) substrates by vapor deposition of Fe (purity 99.99%) using an electron beam evaporator (Omicron, EFM3T). The sample was pulse-magnetized along the Fe [100] easy axis prior to the SPINS and SPMDS measurements. In the SPMDS and SPINS measurements, spectra for the two opposite polarizations of projectiles—i.e., up and down spins—were alternately accumulated more than 100 times to minimize the effect of a change with time. The change of spin (up or down) was controlled by the helicity of the OP radiation [right-hand circular polarization (RHCP) or left-hand circular polarization (LHCP)]. Both SPMDS and SPINS spectra were obtained in the constant pass energy mode at 40 eV.

III. RESULTS AND DISCUSSION

Figure 2 shows INS and MDS spectra on the Fe (100) clean surface. The incident angle of projectiles and exit angle of emitted electrons measured from the surface normal were 45° and 0°, respectively, in both INS and MDS measurements. The INS and MDS spectra are almost the same in Fig. 2. This indicates that the deexcitation mechanisms of He^+ and He^* are basically identical on the Fe (100) clean surface. If the origin of emitted electrons is exactly the same between

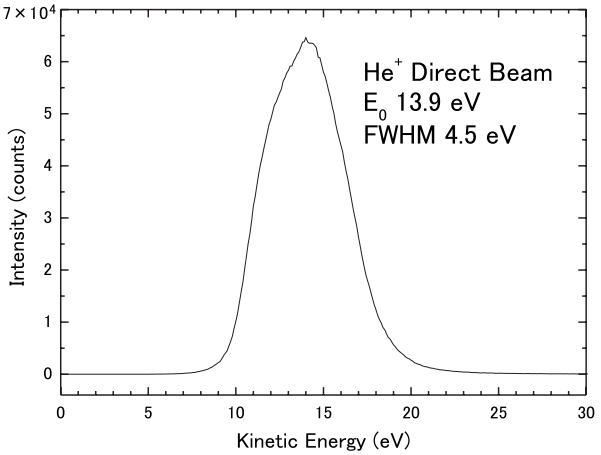

FIG. 3. Energy distribution of the He^+ ion beam used for the INS measurement shown in Fig. 2.

INS and MDS, the spectra should perfectly agree with each other. However, it is noted that the positions of high-energy cutoff are different between INS (~20 eV) and MDS (~17 eV). This disagreement of the high-energy cutoff position between INS and MDS has been consistently observed in our experiments.

In MDS, the kinetic energy of the impinging He^* on the surface is almost thermal (~0.2 eV) so that He^* is reflected by a surface potential [14]. Therefore, all emitted electrons contributing to MDS spectra originate from potential emission—i.e., AN—and kinetic emission does not occur in MDS. In this case, the maximum energy of emitted electrons is expressed as $I_{\mathrm{He}}-\phi-\phi_a$, where I_{He} is the ionization energy of a ground-state He atom, ϕ is the work function of a sample, and ϕ_a is the work function of an analyzer. The effective ionization energy of a He atom may be slightly reduced with an approach to the surface due to image interactions [14]. On the other hand, the kinetic energy distribution of He^+ ions (E_0) in INS has a maximum at about 14 eV with a full width of half maximum of 4.5 eV as shown in Fig. 3. The difference in the high-energy cutoff positions between INS and MDS is attributed to the difference of kinetic energy between He^+ and He^*.

The increase of high-energy cutoffs of emitted electrons induced by slow ions with increasing the ion energy has been observed by several groups [15–17]. Among several proposed mechanisms for the electron emission induced by slow ions, the following two mechanisms are responsible for the increase of high-energy cutoffs with increasing the ion energy observed in the present study.

The first mechanism is energy shift of the He^+ 1*s* vacant level in close encounters of the incident He^+ with target Fe atoms. Then, the maximum kinetic energy of the emitted electron may be larger than that expected for AN of He^* ($I_{\mathrm{He}}-\phi-\phi_a$). Due to their larger kinetic energy, He^+ ions approach to the surface closer than He^*. The close encounter of the He^+ ion causes transient hybridization of the molecular orbital between He^+ and the target. Actually, this transient hybridization of the molecular orbital is well known as the origin of collision-induced neutralization and re-ionization in the ion-surface interaction [18]. The He 1*s* level goes downward as a result of bonding interaction with, for example, Co, Ni, and Cu. Thus, the probability of collision-induced re-ionization of He is negligible on these surfaces [19]. In the *ab initio* Hartree-Fock calculations for the diatomic system of He transition metals by Tsuneyuki and Tsukada, it has been shown that if the *d* orbitals of the target atom are more than half filled, He 1*s* level is lowered due to the bonding interaction of the He 1*s* level with the occupied *d* level [20]. From these experimental and theoretical investigations, it is most likely that the vacant He^+ 1*s* orbital is lowered as it approaches the Fe surface.

The second mechanism of the increase of high-energy cutoffs with increasing ion energy is electronic excitation of surface electrons by moving ions. As discussed by Bixler *et al.* and Juaristi *et al.*, the density of states is distorted from the view of moving projectile ions [16,21]. The effective cutoff is expressed as $m_e(v_F+v_i)^2/2$, where v_F and v_i are the Fermi velocity and incident ion velocity, respectively. In case of the He^+ impact on Fe surfaces with 14 eV, the shift of the effective cutoff energy is estimated to be about 0.4 eV. Since this value is much smaller than that observed in Fig. 2, we infer that the first mechanism mentioned above is the dominant factor for the shift of the high-energy cutoffs.

If we approximate the level shift of He 1*s* to a step function of the internuclear distance between the projectile and the target, the spin asymmetry from raw SPINS data (A_{INS}^{raw}) is

$$A_{INS}^{raw}=\frac{I_{INS}^{\uparrow}+I_{INS}^{\uparrow\prime}-I_{INS}^{\downarrow}-I_{INS}^{\downarrow\prime}}{P_{\mathrm{He+}}(I_{INS}^{\uparrow}+I_{INS}^{\uparrow\prime}+I_{INS}^{\downarrow}+I_{INS}^{\downarrow\prime})}, \tag{4}$$

where I_{INS} is the INS intensity by a He^+ ion whose 1*s* level is identical to that of an isolated He^+ ion while I'_{INS} is that by a He^+ ion whose 1*s* level shifts downward by the bonding interaction as discussed above. Thus, I_{INS} is by He^+ ions located relatively far from the surface, while I'_{INS} is by He^+ ions located relatively near the surface. It is noted that A_{MDS} has a large value above 14 eV (just at the Fermi level) and almost no spin asymmetry appears below 14 eV in SPMDS as described later. This means that $I_{INS}^{\uparrow\prime}$ is almost equal to $I_{INS}^{\downarrow\prime}$ with kinetic energy below 17 eV. Then, $A_{INS}^{raw}\sim(I_{INS}^{\uparrow}-I_{INS}^{\downarrow})/[P_{\mathrm{He+}}(I_{INS}^{\uparrow}+I_{INS}^{\downarrow}+2I'_{INS})]$ in the kinetic energy range below 17 eV. It is clear that the component of I'_{INS} acts as a background for A_{INS}^{raw}. Thus, it is necessary to estimate I'_{INS} in the INS spectrum to estimate A_{INS}.

It is observed that the INS spectrum is almost the same with the MDS spectrum in Fig. 2. This suggests that the energy shift mechanism of INS discussed above is just a minor effect, while the contribution from the energy shift mechanism becomes relatively important in the high-energy region. This feature can be also understood from the relationship between the energy distribution of emitted electrons and the energy separation of levels involved in AN. Indeed, A_{INS}^{raw} agrees with A_{MDS} in the low-energy region (<10 eV) while A_{INS}^{raw} is remarkably reduced in the high-energy region (15–17 eV). Thus, INS and MDS spectra are normalized at the peak position of MDS (3.9 eV), as shown in Fig. 2, and the component obtained from subtraction of MDS from INS is taken as I'_{INS}.

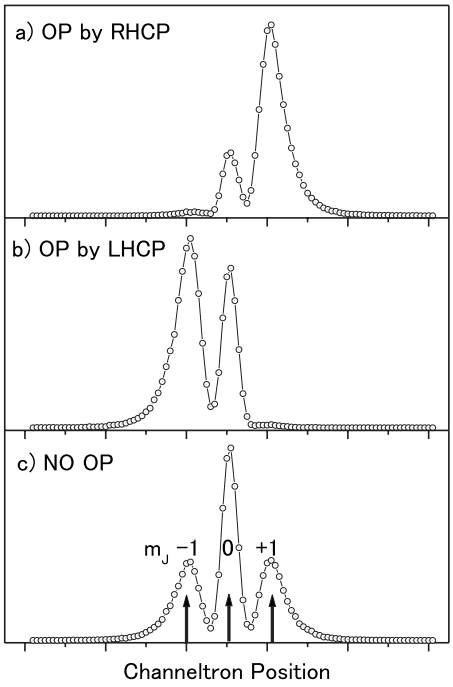

FIG. 4. Stern-Gerlach spectra of He^* optically pumped by RHCP (a), LHCP (b), and without OP (c). The arrows indicate the channeltron positions for magnetic sublevels of He^* (m_J=−1, 0, and +1).

P_{He^*} is expressed as

$$P_{He^*} = \frac{n_+ - n_-}{n_+ + n_0 + n_- + n_s}, \tag{5}$$

where n_+, n_0, and n_- are the density of He^* with a magnetic sublevel (m_J) of +1, 0, and −1, respectively, and n_s is the density of 2 $^1S_0$ atoms. All these values are relatively estimated from Stern-Gerlach measurements as shown in Fig. 4. There are three peaks indicated as m_J=−1, 0, and +1 in the Stern-Gerlach spectra of Fig. 4. Both side peaks (m_J=+1 and −1) are attributed to He^* with m_J=+1 and −1. The center peak (m_J=0) includes both He^* with m_J=0 and 2 $^1S_0$ atoms. From these peak areas, P_{He^*} is finally determined to be 0.72. The difference of P_{He^*} between RHCP and LHCP is due to polarization degree of the OP radiation. P_{He^*} of 0.72 is the averaged value of RHCP and LHCP.

Figure 5 shows A_{MDS} as a function of kinetic energy. The behavior of A_{MDS} exhibits maximum value with positive sign at the Fermi level (~17 eV) while an almost structureless curve is observed below the Fermi level. These features of A_{MDS} are consistent with former studies [22]. It is also shown in Fig. 5 that this behavior of A_{MDS} agrees well with that of A_{INS}. This supports the validity of the estimation procedure of A_{INS} in INS.

The direction of He^* spin can be obtained from Stern-Gerlach measurements. However, there is no established method to determine the direction of He^+ spin. In the present study, the direction of He^+ spin (up or down) was determined from the comparison of sign of A_{INS} and A_{MDS} at the Fermi level.

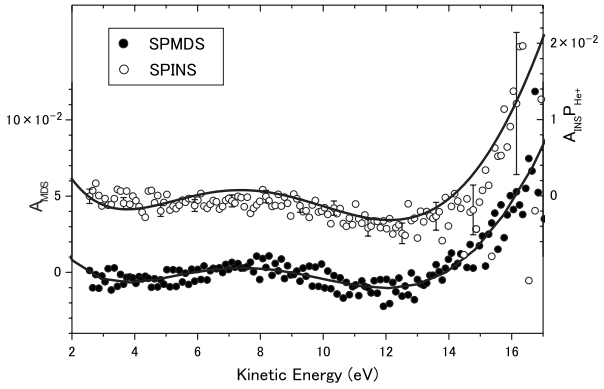

FIG. 5. Spin asymmetry as a function of kinetic energy obtained by spin-polarized He^* (A_{MDS}) and spin-polarized He^+ ($A_{INS}P_{He+}$) together with fitting curves of the fifth-order polynomial.

P_{He^+} is obtained from A_{MDS} and $A_{INS}P_{He^+}$ curves in the following two steps.

(i) The plots of A_{MDS} are fitted by a fifth-order polynomial $f(E)$.

(ii) Then, the plots of $A_{INS}P_{He^+}$ are fitted by a polynomial $kf(E)$, where k (a constant) should be equal to P_{He^+}.

P_{He^+} is finally determined to be 0.19 ± 0.02. The error originates from the fitting procedure for $A_{INS}P_{He^+}$ by the polynomial. In this estimation procedure, P_{He^+} is not substantially influenced by the order number of the fitting polynomial.

The value of P_{He^+} determined in the present study almost agrees with past reports [5,10]. Therefore, the validity of the procedure in the determination of P_{He^+} in these past studies is supported.

It is noted that P_{He^+} is much smaller than other spin-polarized beams as surface probes, such as electrons [23], metastable noble gas atoms (He^*, Ar^*) [24], alkali-metal atoms (Cs) [25], alkali-earth-metal ions (Sr^+) [26], and so on. A partial reason for the small P_{He^+} is depolarization of He^* by the radiation trapping effect in OP [10]. The statistical errors of the spin asymmetry obtained using these probes are in a linear relationship with the reciprocal of the spin polarization of the beam [27]. An improvement of P_{He^+} is needed for possible applications of the spin-polarized He^+ ion beam as a probe for surface and interface spin states.

IV. CONCLUSION

A method to experimentally determine P_{He^+} has been developed. The method is based on a comparison of the spin asymmetry spectra obtained by SPINS and SPMDS. P_{He^*} was obtained from Stern-Gerlach measurements. It was found that the difference of the kinetic energy between He^+ (~14 eV) and He^* (~0.2 eV) causes the difference in the energy position of high-energy cutoff of the spectra between INS and MDS. This difference in the high-energy cutoff of the spectra is mainly interpreted in terms of the energy shift of the He^+ 1s vacant level in a close encounter between He^+ and the target Fe atom. P_{He^+} was finally determined to be 0.19 ± 0.02.

[1] F. J. Kontur, J. C. Lancaster, and F. B. Dunning, Surf. Sci. **600**, 2543 (2006).
[2] T. Suzuki and Y. Yamauchi, Surf. Sci.602, **579** (2008).
[3] J. Leuker, H. W. Ortjohann, R. Zimny, and H. Winter, Surf. Sci. **388**, 262 (1997).
[4] M. Unipan, D. F. A. Winters, A. Robin, R. Morgenstern, and R. Hoekstra, Nucl. Instrum. Methods Phys. Res. B **230**, 356 (2005).
[5] D. L. Bixler, J. C. Lancaster, F. J. Kontrur, R. A. Popple, F. B. Dunning, and G. K. Walters, Rev. Sci. Instrum. **70**, 240 (1999).
[6] T. Suzuki and Y. Yamauchi, Nucl. Instrum. Methods Phys. Res. A **575**, 343 (2007).
[7] D. L. Bixler, J. C. Lancaster, R. A. Popple, F. B. Dunning, and G. K. Walters, Rev. Sci. Instrum. **69**, 2012 (1998).
[8] M. Salvietti, R. Moroni, P. Ferro, M. Canepa, and L. Mattera, Phys. Rev. B **54**, 14758 (1996).
[9] H. D. Hagstrum, Phys. Rev. **96**, 336 (1954).
[10] T. Suzuki and Y. Yamauchi, Nucl. Instrum. Methods Phys. Res. B **256**, 451 (2007).
[11] Y. Yamauchi, M. Kurahashi, and N. Kishimoto, Meas. Sci. Technol. **9**, 531 (1998).
[12] M. Onellion, M. W. Hart, F. B. Dunning, and G. K. Walters, Phys. Rev. Lett. **52**, 380 (1984).
[13] Y. Yamauchi and M. Kurahashi, Appl. Surf. Sci. **169-170**, 236 (2001).
[14] Y. Harada, S. Masuda, and H. Ozaki, Chem. Rev. **97**, 1897 (1997).
[15] H. D. Hagstrum, Y. Takeishi, and D. D. Pretzer, Phys. Rev. **139**, A526 (1965).
[16] D. L. Bixler, J. C. Lancaster, F. J. Kontur, P. Nordlander, G. K. Walters, and F. B. Dunning, Phys. Rev. B **60**, 9082 (1999).
[17] J. C. Lancaster, F. J. Kontur, G. K. Walters, and F. B. Dunning, Phys. Rev. B **67**, 115413 (2003).
[18] H. H. Brongersma, M. Draxler, M. de Ridder, and P. Bauer, Surf. Sci. Rep. **62**, 63 (2007).
[19] R. Souda, T. Aizawa, C. Oshima, S. Otani, and Y. Ishizawa, Phys. Rev. B **40**, 4119 (1989).
[20] S. Tsuneyuki and M. Tsukada, Phys. Rev. B **34**, 5758 (1986).
[21] J. I. Juaristi, M. Rosler, F. J. Garcia de Abajo, H. Kerkow, and R. Stolle, Nucl. Instrum. Methods Phys. Res. B **135**, 487 (1998).
[22] T. Suzuki, M. Kurahashi, and Y. Yamauchi, Surf. Sci. **476**, 63 (2001).
[23] T. Saka, T. Kato, T. Nakanishi, S. Okumi, K. Togawa, H. Horinaka, T. Matsuyama, and T. Baba, Surf. Sci. **454-456**, 1042 (2000).
[24] K. W. Giberson, M. W. Hart, M. S. Hammond, F. B. Dunning, and G. K. Walters, Rev. Sci. Instrum. **55**, 1357 (1984).
[25] E. Torikai, Adv. Colloid Interface Sci. **71**, 317 (1997).
[26] T. Nakajima, N. Yonekura, Y. Matsuo, T. Kobayashi, and Y. Fukuyama, Appl. Phys. Lett. **83**, 2103 (2003).
[27] J. Kessler, *Polarized Electrons* (Springer, Berlin, 1985), p. 245.